Splitting of the $^6S_{5/2}$ state of substitutional Mn^{2+} in $SrCl_2$ by an applied electric field

K. E. Roelfsema
Laboratory for Physical Chemistry, University of Groningen, The Netherlands

H. W. den Hartog
Solid State Physics Laboratory, University of Groningen, The Netherlands

(Received 28 July 1975)

The effect of an applied electric field on the EPR signal of $SrCl_2$:Mn^{2+} was measured at 77°K. The paramagnetic parameters obtained experimentally without an electric field are $b_4 = +1.05 \times 10^{-4}$ cm^{-1}, $A = 82.5 \times 10^{-4}$ cm^{-1}, and $g = 2.0057$. The crystal-field parameter to be introduced in order to explain the observed additional splitting is $b_2^0 = 11.2 \times 10^{-4}$ cm^{-1} for $E = 2.4 \times 10^7$ V/m. The electric field effect which shows axial symmetry about the crystallographic ⟨111⟩ axes, can be explained by a displacement of the Mn^{2+} ion along ⟨111⟩ directions. From a point-ion lattice calculation taking into account the effect of induced dipoles we can estimate the magnitude of this displacement to be $\Delta = 0.11$–0.16 Å for $E = 2.4 \times 10^7$ V/m.

I. INTRODUCTION

Mn^{2+} is a transition ion with a $3d^5$ configuration; the ground state of this ion is usually denoted by $^6S_{5/2}$, which indicates that one is dealing with a pure spin state ($L = 0$) with sixfold degeneracy.

Strontium choloride has a cubic bcc structure with half of the cubes of Cl^- ions being filled with Sr^{2+} ions. The lattice parameter is $d = 6.9767$ Å.

The EPR spectrum has already been studied by Low and Rosenberger[1] at room temperature; their results are in agreement with those presented here. The spectrum can be understood by using the following spin Hamiltonian,

$$\mathcal{H} = g\mu_B \vec{H}\cdot\vec{S} + A\vec{S}\cdot\vec{I} + \tfrac{1}{3}b_4[S_x^4 + S_y^4 + S_z^4 - \tfrac{1}{5}S(S+1) \times (3S^2 + 3S - 1)]. \quad (1)$$

The first term represents the electronic Zeeman energy, the second contribution is the isotropic contact interaction between the electron-spin system and the Mn nucleus; the last term in (1) is the operator equivalent for the cubic-crystal-field potential, which is of the following form:

$$V_c = x^4 + y^4 + z^4 - \tfrac{3}{5}r^4. \quad (2)$$

The crystal field will split the ground-state level; for $SrCl_2$: Mn^{2+} we have a Γ_8 quartet and a Γ_7 doublet with a splitting usually denoted by $3a = 6b_4$. Because $g\mu_B H \gg a$ we expect that all transitions of the type $S_z \leftrightarrow S_z + 1$ will occur and give rise to five lines; on the other hand the hyperfine interaction ($\vec{I}_{Mn} = \frac{5}{2}$) will split each of the lines $S_z \leftrightarrow S_z + 1$ into six equidistant lines. So we expect (because $A \gg a$) six groups of five lines.

The cubic-crystal-field parameter was very small in agreement with the results of Low and Rosenberg.[1] The applied electric field gives rise to extra noncubic-crystal-field parameters in the spin Hamiltonian. The dominant contribution comes from the term corresponding with the parameter b_2^0.

The experimental value of b_2^0 was compared with the theoretically calculated ones as a function of the displacement of the Mn^{2+} ion on basis of a point-charge, point-dipole approximation. From this comparison we have estimated the displacement of the Mn^{2+} ion as a function of the applied electric field.

II. EXPERIMENTAL PROCEDURE

The single crystals of $SrCl_2$: Mn^{2+} were grown from the melt using a modified Bridgeman technique. The starting materials were subjected to special treatments described elsewhere[2] in order to prevent impurities like H_2O, OH^-, and O^{2-} from entering the crystal. The concentration of Mn^{2+} in the crystals was determined by means of an atomic absorption equipment and amounted to typically 300 ppm.

Strontium chloride cleaves along {111} planes and good crystals with a thickness of 1.0 mm or more are easily obtained. Cleavage of the crystals was performed in a dry-box because of the hygroscopic properties of $SrCl_2$. The crystals were mounted on perspex rods with silicone vacuum grease; the orientation of the crystal axes with respect to the magnetic field direction was checked by means of EPR experiments. The measurements were performed with a Varian E3-EPR spectrometer with 100-kHz modulation. The high-voltage supply consisted of a high-voltage transformer, which fed a cascade generator. Voltages up to 25 kV were easily obtained. The electrodes were made of silver foil with a thickness of 25 μm and were stuck to the sides of the sample with the help of silicone vacuum grease. All measurements were performed at liquid-N_2 temperature.

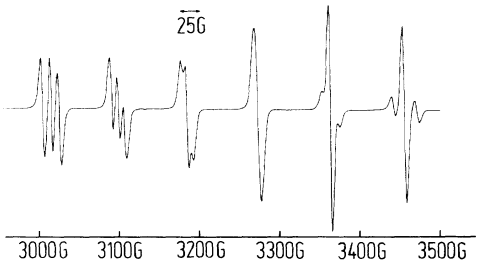

FIG. 1. EPR spectrum of $SrCl_2:Mn^{2+}$ with $\vec{H}_0$ along [100] and $\vec{E}=0$ V/m at 77°K.

III. EXPERIMENTAL RESULTS

In Fig. 1 we show the EPR spectrum of $SrCl_2:Mn^{2+}$ for $\vec{H}_0$ along [100] with $\vec{E}=0$ V/m. We observe six lines associated with the hyperfine interaction of the unpaired-electron configuration and the manganese nucleus. Each of the hyperfine lines is more or less split by the crystal field and the second-order hyperfine interaction. With the help of the exact diagonalization of the first two terms of the Hamiltonian (1),

$$\mathcal{H}=g\mu_B\vec{H}\cdot\vec{S}+A\vec{S}\cdot\vec{I},$$

performed by Wever *et al.*[3] we could calculate the cubic-crystal-field parameter $b_4=1.05\times10^{-4}$ cm^{-1}; $g=2.0057$ and $A=82.5\times10^{-4}$ cm^{-1}. In Fig. 2 we show the EPR spectrum of $SrCl_2:Mn^{2+}$ along [111] with $\vec{E}=0$ V/m and $\vec{E}=2.3\times10^7$ V/m along [111]. The effect of the electric field is clearly observed, it results in a further splitting of each of the hyperfine lines. We shall discuss the reason for this phenomenon in Sec. IV.

In Fig. 3 we show the field dependence of the splitting of the multiplet associated with $M_I=\frac{5}{2}$.

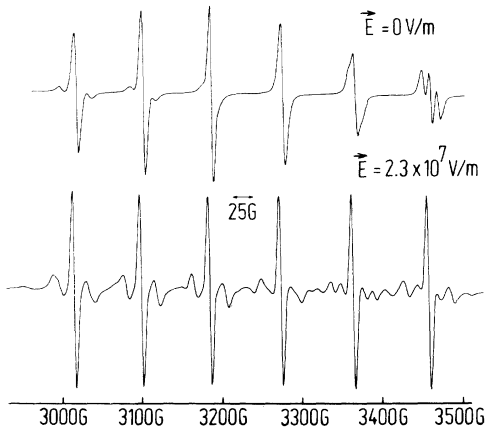

FIG. 2. EPR spectrum of $SrCl_2:Mn^{2+}$ with $\vec{H}_0$ along [111] and $\vec{E}=0$ V/m and with $\vec{E}=2.3\times10^7$ V/m along [111]. $T=77$°K.

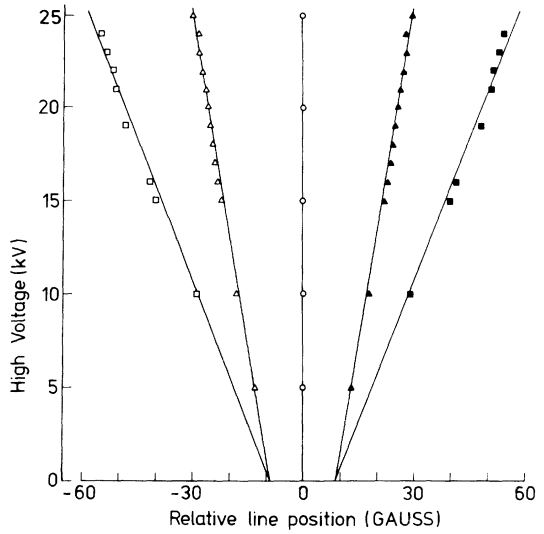

FIG. 3. Behavior of the fine splitting of the $M_I=\frac{5}{2}$ multiplet, as a function of the electric field strength ($\vec{E}\parallel[111]$, $\vec{H}_0\perp[111]$).

We clearly see a linear dependence between the extra splitting and the electric field strength.

In Fig. 4 we show the rotational diagram for transitions associated with $M_I=\frac{5}{2}$ {H_0 is in the $(1\bar{1}0)$ plane and $\vec{E}\parallel[111]$}. We can see that the electric field effect changes when the angle between $\vec{H}_0$ and $\vec{E}$ is changed. When $\vec{H}_0\parallel[001]$ we observed that there is no additional splitting induced by the electric field. So we can conclude that the electric field effect has an angular dependence, which can be described by the familiar $(3\cos^2\theta-1)$ function, where θ is the angle between $\vec{H}_0$ and $\vec{E}$.

In Fig. 5 we show that the additional splitting does not change when $\vec{H}_0$ is rotated in the (111) plane, while the direction of $\vec{E}$ is fixed perpen-

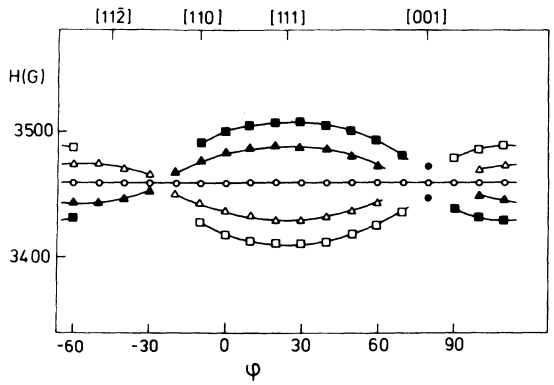

FIG. 4. Fine-structure rotational diagram for the transition associated with $M_I=\frac{5}{2}$; $\vec{H}_0$ is in the $(1\bar{1}0)$ plane and $\vec{E}=2.1\times10^7$ V/m along [111].

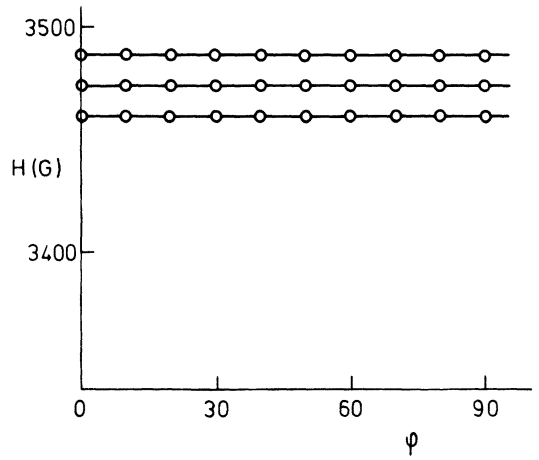

FIG. 5. Rotational diagram for the transition associated with $M_I = \frac{5}{2}$; $\vec{H}_0$ is in the (111) plane and $\vec{E} = 1.7 \times 10^7$ V/m along [111] and perpendicular (111).

dicular to the (111) plane along [111]. Both the crystal-field splitting and the second-order hyperfine splitting are constant, when the sample is rotated about the [111] axis.

Therefore our conclusion is that the electric field effect is axially symmetric about the [111] direction. This confirms our conclusion from Fig. 4 that the electric field effect exhibits a b_2^0-type interaction.

In addition to the experiments mentioned above we have investigated the effect of the electric field, when it is applied along the crystallographic [100] direction. For $\vec{H}_0 \parallel \vec{E}$ we have not been able to detect any electric field effect. However, when $\vec{H}_0 \parallel [111]$ and $\vec{E} \parallel [100]$ an additional splitting is observed, but its magnitude is reduced by a factor 0.55 with respect to the case $\vec{H}_0 \parallel \vec{E} \parallel [111]$.

IV. THEORY

When an ion such as Mn^{2+} is placed in a point-ion lattice the crystal field at the Mn^{2+} position can be expressed in a sum of Coulomb potentials,

$$V(r, \theta, \phi) = \frac{1}{4\pi\epsilon_0} \sum_j \frac{q_j}{|\vec{R}_j - \vec{r}|} , \tag{3}$$

where q_j and $\vec{R}$ are the charge and position vector of the jth ion in the lattice, respectively. With the help of the spherical-harmonic-addition theorem and a Taylor's expansion of the function $1/|\vec{R} - \vec{r}|$ for $R > r$ one can derive the following expressions:

$$V(r, \theta, \phi) = \sum_{n=0}^{\infty} \sum_{m=0}^{n} r^n c_n^m Z_{nm}(\theta, \phi), \tag{4}$$

$$c_n^m = \frac{1}{4\pi\epsilon_0} \sum_{j=1}^{k} \frac{1}{2n+1} q_j \frac{Z_{nm}(\theta_j, \phi_j)}{R_j^{n+1}} \quad \text{for } k \text{ charges}, \tag{5}$$

where the Tesseral harmonic functions Z_{nm} are defined by

$$Z_{n0} = Y_n^0,$$

$$Z_{nm}^c = (1/\sqrt{2})[Y_n^{-m} + (-1)^m Y_n^m] \quad \text{for } m > 0 ,$$

$$Z_{nm}^s = (i/\sqrt{2})[Y_n^{-m} - (-1)^m Y_n^m] \quad \text{for } m > 0 ,$$

where Y_n^m are the familiar spherical harmonic functions. We have followed here the derivation and notation given by Hutchings.[4] The x, y, and z axes are the mutual perpendicular [100], [010], and [001] axes of the crystal lattice. Calculations of the coefficients c_n^m can now be made for all relevant crystal-field parameters taking into account as many of the surrounding ions as will be necessary (10^5 surrounding ions) for convergent results.

We also calculated the crystal-field parameters for positions which were displaced slightly with respect to the origin (the Mn^{2+} position); this implies that under the influence of the static electric field $\vec{E}$ the equilibrium position of the Mn^{2+} impurity is shifted. We have performed these calculations for displacements in the crystallographic [111] direction. The results of these calculations have been compiled in Table I. Only c_2^{-2} is given because $c_2^0 = 0$ and $c_2^2 = 0$ for displacements in the crystallographic [111] direction. c_2^1 and c_2^{-1} are equal in magnitude; it is easy to show that after a rotation of the system of coordinate axes from $\vec{x} \parallel [100]$, $\vec{y} \parallel [010]$, and $\vec{z} \parallel [001]$ to $\vec{x}' \parallel [\bar{1}\bar{1}2]$, $\vec{y}' \parallel [1\bar{1}0]$, $\vec{z}' \parallel [111]$ these potentials transform into one of the type $c_2^{0\prime}$ such that the magnitude of $c_2^{-2} = -c_2^{0\prime}$.

We also calculated the influence of the point dipoles induced by the external electric field and the electric field due to the effective dipole created by the displacement of the central Mn^{2+} impurity. Therefore we derived the following formula (see Appendix) for k dipoles:

$$c_{n\,\mathrm{dip}}^m = \frac{1}{4\pi\epsilon_0} \sum_{j=1}^{k} \frac{4\pi}{2n+1} \frac{(n+1)\,\mu_j \cos\alpha}{R_j^{n+2}} Z_{nm}(\theta_j, \phi_j) , \tag{6}$$

TABLE I. Theoretical second-degree crystal-field parameter calculated for various displacements of the central Mn^{2+} ion.

Δ (Å)	Monop (10^{17} V/m^2)	Dip (10^{17} V/m^2)	Total (10^{17} V/m^2)	b_2^{-2} (10^{-4} cm^{-1})[a]
0.043	−0.53	−0.31	−0.84	−0.19
0.087	−2.13	−1.27	−3.41	−0.76
0.130	−4.83	−2.88	−7.71	−1.73
0.173	−8.65	−5.18	−13.83	−3.10
0.217	−13.66	−8.24	−21.90	−4.90
0.260	−19.91	−12.32	−32.23	−7.21
0.303	−27.49	−16.98	−44.47	−9.95
0.346	−36.50	−22.83	−59.33	−13.28
0.390	−47.05	−30.01	−77.06	−17.24
0.433	−59.26	−38.43	−97.69	−21.86

[a]The values of b_2^{-2} have been calculated using formula (7); it is assumed that $c_2^0/b_2^0 = c_2^{-2}/b_2^{-2}$.

where μ_j is the dipole on the jth lattice position and α is the angle between the dipole vector μ_j and R_j. By definition the vector $\vec{\mu}$ is directed from the negative to the positive charge.

An important feature of the theoretical results is that small displacements of the Mn impurity (of the order of 0.01 Å) will polarize the surrounding lattice to a much larger extent than the external electric field which causes the displacements. A displacement of 0.05 Å of the Mn^{2+} ion along [111] induces dipoles in the surrounding crystal lattice, which produce an electric field at the Mn^{2+} ion that is a factor of 25 stronger than the applied electric field; in this calculation we have used $\alpha_{Cl^-} = 2.96$ Å^3 and $\alpha_{Sr^{2+}} = 1.55$ Å^3 as given by Tessman *et al.*[5] Contributions from dipoles of the first two coordination shells to the crystal-field parameter c_2^{-2} are sufficient for convergent results; in Table I the results for various displacements have been compiled.

According to the coupling mechanism proposed by van Heuvelen,[6] Hagston and Lowther[7] found the following expression for the crystal-field parameter b_2^0:

$$b_2^0 = \frac{3}{125}\,\frac{\xi A_2^0}{W_p}\,[-4R_{++}^2 + 3R_{+-}^2 + R_{--}^2], \tag{7}$$

where $A_2^0 = -e\,c_2^0$, R_{++}^2, R_{+-}^2, and R_{--}^2 are relativistic integrals given by van Heuvelen,[6] $-4R_{++}^2 + 3R_{+-}^2 + R_{--}^2 = 0.0485a_0^2$, $\xi = 260$ cm^{-1}, and $W_p = 30\,500$ cm^{-1}. The theoretical values for b_2^{-2} were calculated for various displacements along the [111] direction and have been compiled in the last column of Table I.

V. DISCUSSION

In the literature up to now some experimental studies have been made on the effect of applied electric fields on the EPR signals due to paramagnetic ions in solids.[8–17] A general feature of the defects showing EPR signals, which depend on the electric field, is a lack of inversion symmetry. When an external electric field is applied to a host crystal of this kind, two different types of centers can be distinguished, the corresponding EPR lines with equal intensities shift into opposite directions. The splitting between the two signals is proportional to the strength of the applied electric field. It can be shown, that the change in energy depends linearly upon the electric field strength. If the site symmetry of the defect includes inversion symmetry the Hamiltonian of the system shows inversion symmetry also. When an electric field is applied in addition to the original Hamiltonian the following term should be included,

$$V = \vec{E}\sum_i q_i \vec{r}_i\,. \tag{8}$$

However, because of the inversion symmetry $\sum_i q_i \vec{r}_i = 0$. When the defect does not show inversion symmetry the dipole operator $\vec{p} = \sum_i q_i \vec{r}_i$ does not vanish generally. It can be shown (see Abragam and Bleaney[20]) that the energy shifts depend linearly upon the expectation value of the dipole operator,

$$\Delta E = \vec{E}\,\langle 0\,|\,\vec{p}\,|\,0\rangle\,, \tag{9}$$

where $|0\rangle$ refers to the ground state of the ion.

Although the Mn^{2+} ions in $SrCl_2$ are built in substitutionally at sites with O_h symmetry we have observed changes in the EPR signals under the influence of external electric fields. This seems to be in contradiction with the reasoning given above. However, another effect of the applied electric field is a small displacement of ions in the crystal lattice which may give rise to changes in the crystal-field Hamiltonian. In our case the applied electric field produces significant contributions to the spin Hamiltonain which do not occur in (1) and (2) and which are of even nature. As it was shown by our experimental results that the additional crystal field has $b_2^0 O_2^0$ character, we must conclude that the symmetry of the Mn^{2+} ions in the presence of the electric field is lower than O_h.

For crystalline hosts in which the Mn^{2+} ions occupy sites with lower symmetry even without the application of the external electric field, there can be a crystal-field term $b_2^0 O_2^0$ in the spin Hamiltonian. In these materials the application of an electric field results in a splitting of the spectrum as shown by the work of Kiel and Mims.[9–16] Our experimental results for Mn^{2+} in $SrCl_2$ only show an additional shift of the various $S_z \rightarrow S_z + 1$ transitions which, because of the O_h-site symmetry of the transition-metal impurity, is due to a displacement of the Mn^{2+} ion. Displacements as discussed here have been considered before by Dreybrodt *et al.*[18,19] for Mn^{2+}-vacancy complexes in NaCl crystals. These authors found that displacements of ions surrounding the impurity also give rise to even contributions to the crystal-field Hamiltonian. Although Dreybrodt and Silber[19] conclude that the displacement of the central Mn^{2+} ion does not produce significant contributions to the additional crystal-field Hamiltonian, their results strongly suggest that in some cases an external electric field of $(1-2)\times 10^7$ V/m may induce significant changes of the equilibrium positions of ions in crystals.

The rotational diagrams given in Figs. 4 and 5 show that we are dealing with a center having axial symmetry; the symmetry axis for $\vec{E} \parallel [111]$ is along [111]. From the positions of the ions in the surrounding cubic $SrCl_2$ lattice, it is easy to see that a deformation due to the electric field could lead to a site with C_{3v} symmetry.

TABLE II. Second-degree crystal-field parameter for various electric field strengths. $\vec{E} \parallel [111]$.

E (10^7 V/m)	b_2^0 (10^{-4} cm^{-1})
1.0	5.1
1.5	7.7
2.0	9.7
2.4	11.2

An obvious explanation for the observed shifts of the EPR lines is a displacement of the Mn impurity, which lowers the symmetry from O_h to axial symmetry. This leads to extra contributions to the crystal-field spin Hamiltonian,

$$\mathcal{H}^* = \tfrac{1}{3}b_2^0O_2^0 + \tfrac{1}{60}b_4^0O_4^0 + \tfrac{1}{60}b_4^3O_4^3 + \tfrac{1}{60}b_4^4O_4^4 . \qquad (10)$$

Here, the z axis is chosen along the symmetry axis of the crystal-field Hamiltonian; for C_{4v} symmetry $b_4^3 = 0$. The variations of the spectra as compared to the cubic spectrum were considered, and we found that the shift of the EPR lines is approximately linear in M_S. This behavior is characteristic for a second-degree crystal field, implying that for a first approximation we can assume that the extra crystal field resulting from the electric field is of the form $\frac{1}{3}b_2^0O_2^0$. From the results given in Fig. 3 we can calculate the values of b_2^0 for various magnitudes of the electric field. Some of the results have been compiled in Table II.

The measurements presented in Sec. III show, that maximum additional crystal-field splitting is obtained when $\vec{E} \parallel \langle 111 \rangle$. This indicates that the displacements take place preferentially along $\langle 111 \rangle$. In order to obtain more information about the details of the displacements let us consider the results for $\vec{E} \parallel [111]$ and $\vec{E} \parallel [100]$. We have seen that there is axial symmetry about the [111] axis when the electric field is applied along [111]. For a spherical-symmetry situation one would, for $\vec{E} \parallel [100]$, also expect axial symmetry about the [100] axis and a maximum additional crystal-field splitting for $\vec{H}_0 \parallel [100]$. This, however, has not been observed; when $\vec{E} \parallel [100]$ and $\vec{H}_0 \parallel [100]$ no extra splitting due to the external electric field could be found. Like $\vec{E} \parallel [111]$ we found that for $\vec{E} \parallel [100]$ maximum crystal-field splitting is observed for $\vec{H}_0 \parallel [111]$! The magnitude of the electric field-induced splitting is a factor of 0.55 smaller for $\vec{E} \parallel [100]$ than for $\vec{E} \parallel [111]$, which is approximately equal to the factor $\cos\theta = \frac{1}{3}\sqrt{3}$; θ is the angle between [100] and [111]. These experimental facts provide strong evidence for our interpretation that the displacement of the Mn^{2+} ions can take place only along [111]. This can be understood by considering the cubic-crystal-field potential of the Mn^{2+} site, which has the form given in formula (2). When looking at a sphere centered at the Mn nucleus, maxima and minima of this potential are found in the crystal $\langle 100 \rangle$ and $\langle 111 \rangle$ directions, respectively. We expect that the displacement of the Mn^{2+} ion will be into the directions with minimum energy, implying that the cubic-crystal-field parameter b_4 is positive. This is consistent with results on CaF_2: Mn^{2+}; (see Low[21] p. 118).

The theoretical calculations for $b_2^{\bar{2}}$ ($= b_2^0$ in the coordinate system with $\vec{z} \parallel [111]$) show that for an external field of 2.3×10^7 V/m we find a displacement of approximately 0.32 Å, which is rather large but not unrealistic. It was found by Hagston and Lowther[7] that the theoretically calculated values according to formula (7) for the second-degree crystal-field parameters of the spin Hamiltonian are usually too low by a factor of two to three. When a correction for this phenomenon is applied we find displacements of typically 0.11–0.16 Å.

In conclusion we propose, that it is possible to displace loose impurities in ionic crystals under the influence of external electric fields of moderate strengths.

ACKNOWLEDGMENT

The authors are grateful to P. Wesseling for growing the crystals.

APPENDIX

We start with the formula derived for k point charges in the lattice,

$$V(r, \theta, \phi) = \sum_{n=0}^{\infty}\sum_{m=0}^{n} r^n c_n^m Z_{nm}(\theta, \phi) ,$$

$$c_n^m = \frac{1}{4\pi\epsilon_0}\sum_{j=1}^{k}\frac{4\pi}{2n+1} q_j \frac{Z_{nm}(\theta_j, \phi_j)}{R_j^{n+1}} .$$

For one charge we have

$$c_n^m = \frac{1}{4\pi\epsilon_0}\frac{4\pi}{2n+1} q_j \frac{Z_{nm}(\theta_j, \phi_j)}{R_j^{n+1}} .$$

Considering a dipole of strength $q\,2\delta$ in Q we find at position P

$$c_n^m = \frac{1}{4\pi\epsilon_0}\frac{4\pi}{2n+1}\left(\frac{q_j Z_{nm}(\theta_j, \phi_j)}{(R_j - \delta\cos\alpha)^{n+1}} - \frac{q_j Z_{nm}(\theta_j, \phi_j)}{(R_j + \delta\cos\alpha)^{n+1}}\right),$$

$$= \frac{1}{4\pi\epsilon_0}\frac{4\pi q_j R_j^{n+1}}{(2n+1)(R_j^2 - \delta^2\cos^2\alpha)^{n+1}}$$

$$\times\left[\left(1 + \frac{\delta\cos\alpha}{R_j}\right)^{n+1} - \left(1 - \frac{\delta\cos\alpha}{R_j}\right)^{n+1}\right] Z_{nm}(\theta_j, \phi_j) .$$

With the help of the binomial expansion we find up to third order,

$$c_n^m = \frac{1}{4\pi\epsilon_0}\frac{4\pi q_j R_j^{n+1}}{(2n+1)(R_j^2 - \delta^2\cos^2\alpha)^{n+1}}$$

$$\times 2(n+1)\frac{\delta\cos\alpha}{R_j} Z_{nm}(\theta_j, \phi_j).$$

If $\delta \ll R$ this leaves

$$c_n^m = \frac{1}{4\pi\epsilon_0} \frac{4\pi(n+1)}{2n+1} \frac{2q_j\delta\cos\alpha\, R_j^{n+1}}{R_j^{2n+2}R_j} Z_{nm}(\theta_j, \phi_j),$$

and finally with $\mu_j = 2q_j\delta$ we find for k dipoles

$$c_n^m = \frac{1}{4\pi\epsilon_0} \sum_{j=1}^{k} \frac{4\pi(n+1)}{2n+1} \frac{\mu_j\cos\alpha}{R_j^{n+2}} Z_{nm}(\theta_j, \phi_j),$$

where $\vec{\mu}_j$ is by definition the vector directed from the negative to the positive charge, and α is the angle between $\vec{\mu}_j$ and $\vec{R}_j$, where the direction of $\vec{R}_j$ is from Q to P.

[1]W. Low and U. Rosenberger, Phys. Rev. 116, 621 (1959).
[2]H. W. den Hartog, P. Mollema, and A. S. Schaafsma, Phys. Status Solidi B 55, 72 (1973).
[3]H. Wever, D. I. M. Knottnerus, and H. W. den Hartog (unpublished).
[4]M. T. Hutchings, in *Solid State Physics*, edited by F. Seitz and D. Turnbull (Academic, New York, 1964), Vol. 16.
[5]J. R. Tessman, A. H. Kahn, and W. Shockley, Phys. Rev. 92, 890 (1953).
[6]A. van Heuvelen, J. Chem. Phys. 46, 4903 (1967).
[7]W. E. Hagston and J. E. Lowther, J. Phys. Chem. Solids 34, 1773 (1973).
[8]G. W. Ludwig and H. H. Woodbury, Phys. Rev. Lett. 7, 240 (1961).
[9]F. S. Ham, Phys. Rev. Lett. 7, 242 (1961).
[10]W. B. Mims, Phys. Rev. 140, A531 (1965).
[11]A. Kiel, Phys. Rev. 148, 247 (1966).
[12]A. Kiel and W. B. Mims, Phys. Rev. 153, 378 (1967).
[13]A. Kiel and W. B. Mims, Phys. Rev. B 1, 2935 (1970).
[14]A. Kiel and W. B. Mims, Phys. Rev. B 3, 2878 (1971).
[15]A. Kiel and W. B. Mims, Phys. Rev. B 5, 803 (1972).
[16]A. Kiel and W. B. Mims, Phys. Rev. B 6, 34 (1972).
[17]T. Rs. Reddy, Phys. Lett. A 36, 11 (1971).
[18]W. Dreybrodt and G. Pfister, Phys. Status Solidi 34, 69 (1969).
[19]W. Dreybrodt and D. Silber, Phys. Status Solidi 34, 559 (1969).
[20]A. Abragam and B. Bleaney, in *Electron Paramagnetic Resonance of Transition Ions* (Clarendon, Oxford, 1970).
[21]W. Low, in *Supplement to Solid State Physics*, edited by F. Seitz and D. Turnbull (Academic, New York, 1960).